Dark soliton dynamics and interactions in continuous-wave-induced lattices

Ilias Tsopelas, Yannis Kominis, and Kyriakos Hizanidis
School of Electrical and Computer Engineering, National Technical University of Athens, Zographou 15773, Greece
(Received 21 December 2006; revised manuscript received 30 May 2007; published 22 October 2007)

The dynamics of dark spatial soliton beams and their interaction under the presence of a continuous wave (CW), which dynamically induces a photonic lattice, are investigated. It is shown that appropriate selection of the characteristic parameters of the CW result in controllable steering of a single soliton as well as controllable interaction between two solitons. Depending on the CW parameters, the soliton angle of propagation can be changed drastically, while two-soliton interaction can be either enhanced or reduced, suggesting a reconfigurable soliton control mechanism. Our analytical approach, based on the variational perturbation method, provides a dynamical system for the dark soliton evolution parameters. Analytical results are shown in good agreement with direct numerical simulations.

DOI: 10.1103/PhysRevE.76.046609 PACS number(s): 42.65.Tg, 42.65.Sf

I. INTRODUCTION

Spatial and temporal dark solitons in planar waveguides and bulk media have been the subject of intense theoretical and experimental studies in recent years [1–3]. Dark solitons can be formed in optical media having opposite sign of dispersion or diffraction and Kerr nonlinearity, as the effects of these two mechanisms on the pulse or beam shape, under propagation, are balanced, resulting in robust dark soliton evolution. In comparison with bright ones, spatial dark solitons provide an alternative potentiality in photon management applications, since they have qualitatively different properties (i.e., phase jump in beam center constitutes an additional invariant of the dark soliton propagation) [1]. In the context of all-optical processing, and more specifically in switching and controlled beam steering applications, dark solitons exhibit advantageous performance in comparison with bright ones under the presence of material loss, noise, or perturbations. Moreover, the interaction forces between dark solitons appear to be less drastic than those of bright beams, resulting in stable two-soliton evolution [1,2,4].

The underlying model of spatial soliton propagation in a Kerr-type defocusing medium is the nonlinear Schrödinger (NLS) equation,

$$i\frac{\partial u}{\partial Z}+\frac{1}{2}\frac{\partial^2 u}{\partial X^2}-|u|^2u=0, \tag{1}$$

where X and Z are the transverse and the longitudinal dimensions normalized to the characteristic size of the beam and to the diffraction distance, respectively, while u is the normalized beam amplitude.

Dark soliton solutions of the integrable Eq. (1) (known as NLS$^+$) have been derived with utilization of the inverse scattering transform (IST) method for the cases of single [5] and multiple [6] soliton propagation. Additionally, quite recent studies are focused on the analysis of perturbation-induced dynamics of dark solitons as well as on the development of perturbation methods including Hamiltonian approaches [7], direct perturbation analysis [8–14], variational approaches [15], and IST-based methods [16].

On the other hand, the research interest in the propagation of dark solitary waves and localized excitations in nonlinear photonic lattices and waveguide arrays have significantly increased during the last years, from both the theoretical [17–21] and the experimental point of view [22–25], as the evolution of spatial beams in periodic materials has a rich set of interesting features that have no counterpart in the case of homogeneous waveguides, e.g., dark excitations have been experimentally observed in the normal diffraction regime in self-focusing optical lattices [22]. Furthermore, dynamically induced photonic lattices (periodic structures modulated by a control optical signal) have been recently proposed [22,24,26,27] for applications related to reconfigurable dynamical control of dark soliton beams. Moreover, the control signal, which forms the periodic potential, can also affect the mutual interaction (attractive or repulsive) force of two dark beams propagating in the same medium. Quite recently, bright soliton dynamics under the presence of a linear periodic wave were studied [28–31] analytically and numerically in planar [28,30,31] and bulk [29] media. In the aforementioned studies, a control signal in the form of either a continuous wave (CW) or a more general linear dispersive periodic wave (PW) has been considered.

In this work, we study dark soliton dynamics and interactions under the presence of a CW, which dynamically modulates the properties of the defocusing nonlinear waveguide through the intensity-dependent refractive index. We demonstrate that efficient beam steering is achieved by the injection of the original dark soliton beam in an appropriately designed CW-induced photonic lattice, while we underline the qualitatively different performance of dark beams propagating in a periodic lattice, with respect to bright ones. Our analytical results are based on a variational perturbation method using the Lagrangian formalism [15]. The analytical results are shown in remarkable agreement with the corresponding direct numerical simulations. Radiation modes are not included in our analysis, as they appear in limited cases (under strong perturbation or for the case of a CW with zero transverse velocity). In addition, different evolution scenarios of two initially well-separated dark soliton beams under the presence of a CW show that the presence of the CW control signal crucially determines (enhances or reduces) the mutual interaction between the two beams.

II. SINGLE SOLITON DYNAMICS

The NLS$^+$ Eq. (1) for self-defocusing media has the stable CW solution

$$u = u_0 \exp(-iu_0^2 Z) \tag{2}$$

while the same equation admits the well-known dark soliton solution

$$u_s(X,Z) = u_0\{B \tanh[u_0 B(X-\nu Z)] + iA\}\exp(-iu_0^2 Z), \tag{3}$$

where $A=\nu/u_0$ and $A^2+B^2=1$. On the other hand, a low amplitude CW having the following form:

$$u_{cw}(X,Z) = a \exp\{-i[k_X X + (1/2)k_X^2 Z + \phi]\}, \tag{4}$$

is a solution of the linear Schrödinger equation,

$$i\frac{\partial u_{cw}}{\partial Z} + \frac{1}{2}\frac{\partial^2 u_{cw}}{\partial X^2} = 0, \tag{5}$$

where the nonlinear term is considered negligible. Following the same approach as in Refs. [28–31], the superposition of the dark soliton and the CW is considered,

$$u = u_s + u_{cw}. \tag{6}$$

It is worth mentioning that, for the case of self-defocusing medium, a constant amplitude wave is modulationally stable, under propagation. Hence we may consider that the CW control signal remains unaffected by the presence of the dark soliton, while it is the dark soliton evolution that is modified due to the CW. The latter is also confirmed by the direct numerical simulations shown in the following sections.

The substitution of Eq. (6) in the NLS$^+$ Eq. (1) results in a nonlinear term of the form

$$|u|^2 u = |u_s|^2 u_s + u_s^2 u_{cw}^* + 2|u_s|^2 u_{cw} + 2u_s|u_{cw}|^2 + u_{cw}^2 u_s^* + |u_{cw}|^2 u_{cw}. \tag{7}$$

By considering a CW having small amplitude (e.g., smaller than 10% of the soliton dark deep), we can neglect terms that are second and third order in u_{cw}, and obtain the following perturbed NLS$^+$ equation:

$$i\frac{\partial u_s}{\partial Z} + \frac{1}{2}\frac{\partial^2 u_s}{\partial X^2} - |u_s|^2 u_s = R(u_s, u_{cw}), \tag{8}$$

where

$$R(u_s, u_{cw}) = (u_s^2 u_{cw}^* + 2|u_s|^2 u_{cw}) \tag{9}$$

is the perturbation term, which takes into account the modification of dark soliton propagation due to the presence of a CW. Next, in the perturbed NLS$^+$ Eq. (8) we substitute the renormalized wave field with $u_0>0$:

$$u_s = u_0 v \exp(-iu_0^2 Z), \tag{10}$$

and we obtain the perturbed NLS$^+$ equation in a renormalized form. Setting $u_0=1$, the renormalized NLS$^+$ equation can be written as

$$i\frac{\partial v}{\partial Z} + \frac{1}{2}\frac{\partial^2 v}{\partial X^2} - (|v|^2 - 1)v = R(v, u_{cw}), \tag{11}$$

where

$$R(v, u_{cw}) = a[\exp(i\phi_1)v^2 + 2\exp(-i\phi_1)|v|^2] \tag{12}$$

with $\phi_1 = k_X X + (\frac{1}{2}k_X^2 - 1)Z + \phi$.

In order to study the perturbed NLS$^+$ equation, we apply a variational method based on the Lagrangian formalism of Ref. [15]. Accordingly, the total Lagrangian density $\mathcal{L}$ can be expressed as $\mathcal{L}(v) = \mathcal{L}_0(v) + \Delta\mathcal{L}(v)$, where

$$\mathcal{L}_0(v) = \frac{i}{2}\left(v^*\frac{\partial v}{\partial Z} - v\frac{\partial v^*}{\partial Z}\right)\left(1 - \frac{1}{|v|^2}\right) - \frac{1}{2}\left|\frac{\partial v}{\partial X}\right|^2 - \frac{1}{2}(|v|^2 - 1)^2 \tag{13}$$

and

$$\Delta\mathcal{L}(v) = 2a\,\mathrm{Re}[\exp(i\phi_1)v]|v|^2. \tag{14}$$

By using the following ansatz:

$$v(X,Z) = \{B\tanh[B(X - X_0)] + iA\}, \tag{15}$$

with $B>0$, the averaged Lagrangian density $L(v) = \int_{-\infty}^{+\infty}\mathcal{L}(v)dX$ takes the form

$$L(v) = 2\frac{dX_0}{dZ}\left[-AB + \tan^{-1}\left(\frac{B}{A}\right)\right] - \frac{4}{3}B^3 + 2a\frac{\pi \sin\phi_2}{\sinh[\pi k_X/(2B)]}[k_X^2/2 + Ak_X - 1] - 4aA\pi\delta(k_X)\sin(\phi_2), \tag{16}$$

where $\phi_2 = k_X X_0 + (\frac{1}{2}k_X^2 - 1)Z + \phi$.

The term of Eq. (16), containing the Dirac's delta function $\delta(k_X)$, results from the integration of a term of the $\mathcal{L}$ function, which depends sinusoidally on the transverse coordinate X. For the calculation of this diverging integral, the Cauchy principal value has been taken into account; the validity of such a consideration is shown to be confirmed by the following numerical simulations of the original Eq. (1). This singular dependence of the averaged Lagrangian density on the transverse velocity of the CW (k_X) represents a resonance between the transverse wave numbers of the CW and the dark soliton, with the latter considered as being zero through this work, without loss of generality. This drastic dependence of the averaged Lagrangian on the resonance condition excludes the range of values of the transverse wave number of the CW (k_X) around zero from the domain of applicability of the variational method. A qualitative differentiation of the results of perturbation analysis, in the vicinity of resonances, is a common feature of perturbation methods used in many physical problems and actually it also occurs in the related problem of bright soliton interactions with CW, where it has been shown that the dynamical system governing the evolution of the soliton's parameters under propagation have a reduced number of degrees of freedom for the resonant case $k_X=0$ [30], in comparison to the dynamical system obtained for the case $k_X \neq 0$ [28].

A. Nonzero transverse velocity CW ($k_X \neq 0$)

In this case we can neglect the $\delta(k_X)$ term of Eq. (16), and the application of the Euler-Lagrange equations to the aver-

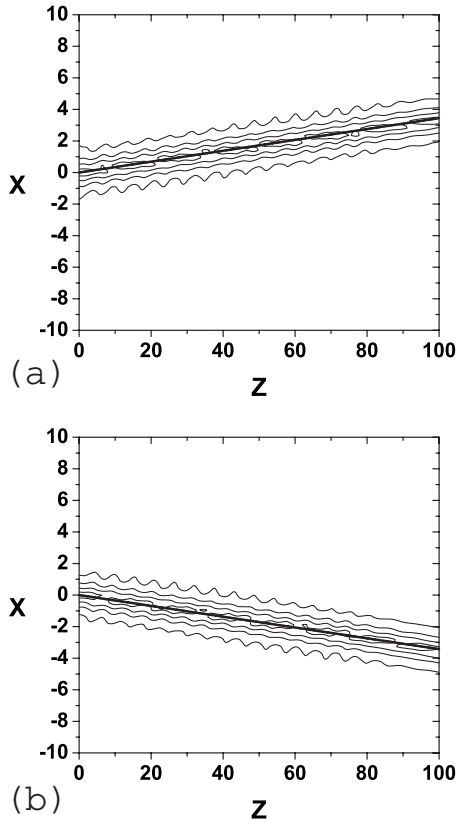

FIG. 1. Displacement of a dark soliton (beam steering) in a CW-induced photonic lattice with $k_X=1$, $a=0.05$ and phase (a) $\phi=\pi/2$ and (b) $\phi=-\pi/2$. The thick line depicts results from the variational method.

aged Lagrangian L, utilizing also the relation $A^2+B^2=1$, leads to the following dynamical system, governing the evolution of the dark soliton's parameters, under propagation:

$$\frac{dA}{dZ} = \frac{-2a\pi k_X \cos\phi_2}{4B}\left[\frac{k_X^2/2 + Ak_X - 1}{\sinh(\pi w)}\right], \tag{17}$$

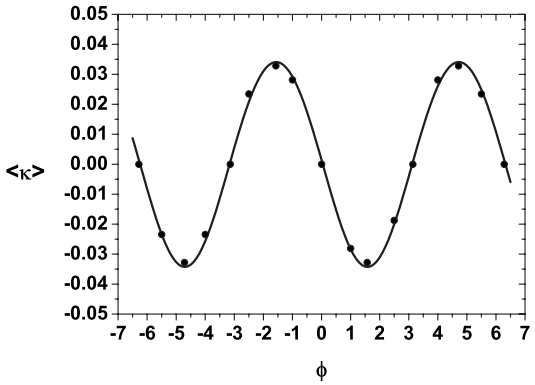

FIG. 2. Dependence of the soliton mean transverse velocity $\langle\kappa\rangle$ on the CW phase ϕ. The solid line depicts results from the variational method, while black dots represent results from direct simulations; $X_0=0$, $k_X=1$, $a=0.05$.

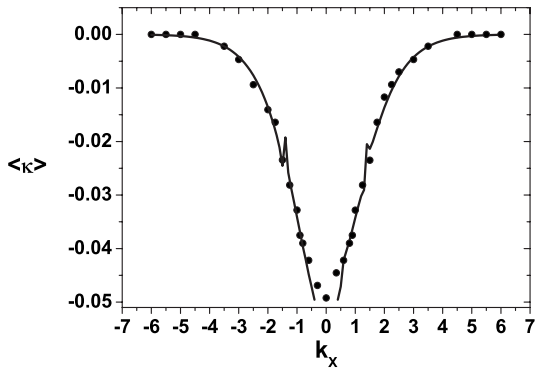

FIG. 3. Dependence of the soliton mean transverse velocity $\langle\kappa\rangle$ on the CW transverse velocity k_X; $X_0=0$, $\phi=\pi/2$, $a=0.05$.

$$\frac{dX_0}{dZ} = A - \frac{Aa\pi\sin\phi_2}{2B^2}\left[\frac{-B/Ak_X}{\sinh(\pi w)} + \frac{\frac{\pi k_X}{2B^2}(k_X^2/2 + Ak_X - 1)}{\tanh(\pi w)\sinh(\pi w)}\right] \tag{18}$$

with $w=k_X/(2B)$, $\phi_2=k_XX_0+\left(\frac{1}{2}k_X^2-1\right)Z+\phi$, and k_X, $A\neq 0$, and $B>0$. This is a nonlinear, nonautonomous system derived under no assumption on the length scales of the beam width and the CW period similarly to the bright soliton-CW interaction case [28]. The equations describing the transverse velocity and the beam center displacement of the soliton are coupled in contrast to previous studies [32], where length scale separation resulted in a simplified system. The results of the variational perturbation method are obtain directly from the dynamical system (17) and (18), while the numerical results, presented in the following, are obtained by considering as an initial condition ($Z=0$) the superposition of both the original dark soliton beam of Eq. (3) and the control signal of Eq. (4).

As it has been demonstrated in previous works [28,29,31], from the point of view of potential applications to reconfigurable soliton control, a nonzero transverse velocity $k_X\neq 0$ of the CW control signal offers advanced potentiality in optical processing. In this case, the CW transfers momentum to the dark soliton leading to controllable drift and steering of the latter, as in the bright soliton-CW (or -PW) interaction case

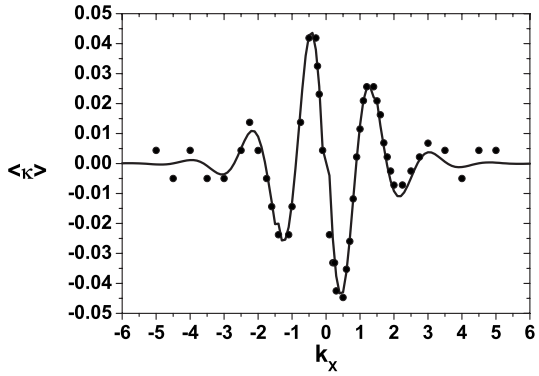

FIG. 4. Dependence of the soliton mean transverse velocity $\langle\kappa\rangle$ on the CW transverse velocity k_X; $X_0=3.5$, $\phi=0$, $a=0.05$.

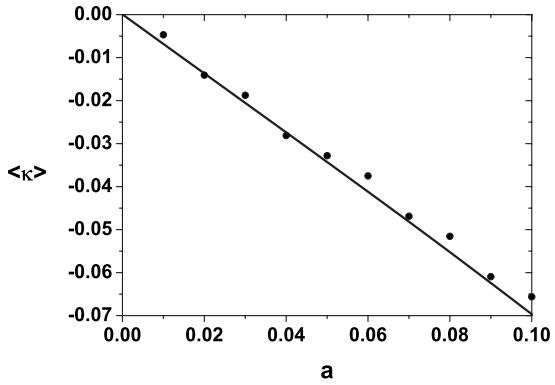

FIG. 5. Dependence of the soliton mean transverse velocity $\langle\kappa\rangle$ on the CW amplitude a; $X_0=0$, $k_X=1$ and $\phi=\pi/2$.

[28,29,31]. In the following, the dependence of the CW-induced soliton mean transverse velocity on the CW parameters [amplitude (a), transverse velocity (k_X), and phase (ϕ)] is investigated. Additionally, the qualitative differences between dark and bright beam propagation in dynamically photoinduced lattices are emphasized. In the examples that follow, we choose appropriate values for the parameters of the CW and/or the initial soliton position, with respect to the CW, corresponding to maximum soliton beam displacement.

Figure 1 depicts the propagation of a dark soliton (we use the initial conditions of a black soliton: $B=1$, $A=0$, $u_0=1$, $X_0=0$ at $Z=0$) for the cases of a CW having amplitude $a=0.05$, transverse velocity $k_X=1$, and phase (a) $\phi=\pi/2$, and (b) $\phi=-\pi/2$. The contour plots of Figs. 1(a) and 1(b), obtained from direct numerical integration of the NLS Eq. (1), depict the absolute value of the amplitude of the superposition of both soliton beam and CW ($|u|$), while the thick lines, provided by the variational approximation, depict the displacement of the dark soliton beam under propagation (X_0). It is evident that numerical and analytical results are in agreement, showing that efficient beam steering is achieved by varying the phase difference between the dark beam and the control signal. It is worth mentioning that, even though fast amplitude (and width) beam oscillations are observed [as in the bright soliton-CW (or -PW) interaction case], both numerical and analytical results provide constant transverse velocity with no small scale oscillations.

Moreover, as shown in Fig. 2, the mean soliton transverse velocity $\langle\kappa\rangle=X_0(Z_{\max})/Z_{\max}$, related to the total displacement of the center X_0 of the spatial soliton beam [28], depends strongly on the initial phase difference between the dark soliton and the CW control signal. The latter can be practically controlled, for example, by changing the difference of the optical paths of the two waves from a common source to the launching point where they are superimposed. The corresponding curve is symmetric with respect to the origin (odd function) and has a sinusoidal profile with period 2π, showing that an appropriate choice of the CW phase determines both the sign and the magnitude of $\langle\kappa\rangle$. A similar plot may be obtained by keeping the CW parameters fixed and varying the initial soliton position X_0.

As it is already known for the case of bright solitons [28,29,31], the transverse velocity (k_X) of the CW is also crucial for the mean induced velocity $\langle\kappa\rangle$ of the dark soliton. However, unlike bright soliton-CW interactions, in the case of dark solitons with a zero initial position [$X_0(Z=0)=0$], the corresponding curve is symmetric with respect to the $k_X=0$ vertical axis, meaning that by varying only the transverse velocity of the CW, we may control only the angle of soliton beam center displacement, but not its direction (Fig. 3). Maximum transverse velocity of the dark soliton occurs around $k_X=0$. However, this is also the range of values of k_X, where the maximum divergence between analytical and numerical results takes place, as expected due to the presence of the singular term $\delta(k_X)$ in the averaged Lagrangian (16). Actually, the presence of this singular term excludes a small area around $k_X=0$ from the domain of applicability of the dynamical system (17) and (18); as a result the corresponding curve consists of two branches which decrease rapidly as approaching $k_X=0$. Also, note that the local jumps of this curve at the points $k_X=\pm\sqrt{2}$ manifest a bifurcation of the

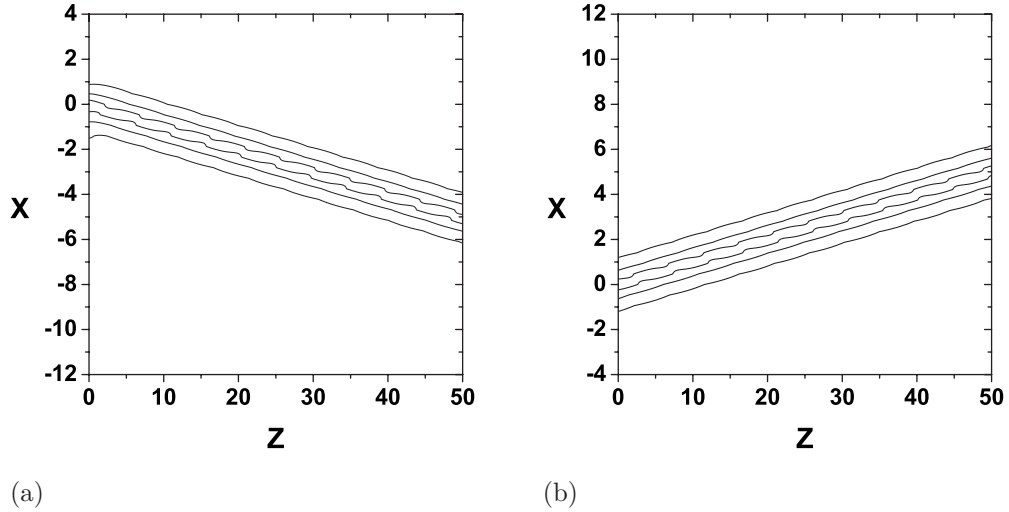

FIG. 6. By varying the CW phase from (a) $\phi=0$ to (b) $\phi=\pi/2$ the dark soliton beam obtains different mean transverse velocity $\langle\kappa\rangle$; $k_X=0$, $a=0.10$.

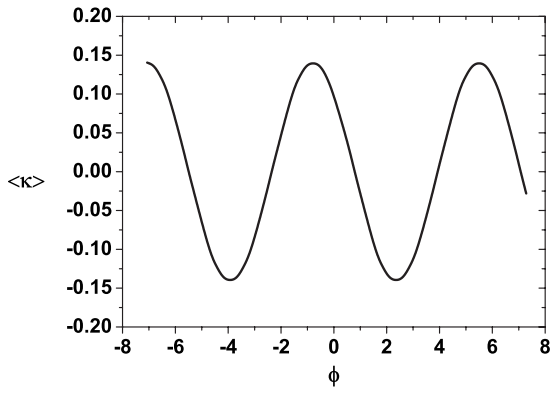

FIG. 7. Dependence of soliton mean transverse velocity $\langle\kappa\rangle$ on the CW phase (ϕ); $k_X=0$, $a=0.10$.

underlying dynamical system: for these specific values of k_X ($k_X=\pm\sqrt{2}$ for $u_0=1$), the Z dependence of the phase parameter ϕ_2 of Eqs. (17) and (18) is eliminated resulting in a lower degree of freedom dynamical system for the evolution parameters.

By selecting a nonzero initial value for the soliton beam center $[X_0(Z=0)\neq 0]$, and varying CW transverse velocity (k_X), we may control both the sign and the magnitude of soliton velocity $\langle\kappa\rangle$, as it can be seen in Fig. 4. This curve is antisymmetric with respect to the origin. Similar results have been found in bright soliton-CW interactions (having zero initial position) in one-dimensional [28] and two-dimensional [29] self-focusing media, but in the case of a dark soliton several local extrema are present, while the sign of the dark beam velocity can be different even for two CW velocities having the same sign. Hence soliton velocity $\langle\kappa\rangle$ dependence on k_X for a dark beam with nonzero initial position resembles the case of a bright soliton (with zero initial position) propagating in a PW-induced lattice [31].

Finally, by keeping all CW parameters fixed and varying the amplitude of the control signal, as expected, we can only control the magnitude of the resulting soliton mean transverse velocity (Fig. 5). The $\langle\kappa\rangle$ dependence on CW amplitude (a) is linear and the slope of the corresponding curve is determined by the remaining CW parameters.

B. Zero transverse velocity CW ($k_X=0$)

We investigate this case by applying numerical integration of the original Eq. (1) and using a dark soliton beam with zero initial transverse velocity ($A=0$), unitary background ($u_0=1$), and amplitude ($B=1$), and zero initial beam center position ($X_0=0$). Our numerical investigation indicates that the dark soliton beam, under the presence of a CW with $k_X=0$, evolves as a breathing type dark solitary wave undergoing amplitude (width) and chirp oscillations. This behavior is similar to the one bright solitons interacting with linear waves exhibit [28,30,31]. On the other hand, unlike bright solitons, dark beams interacting with CW obtain a constant nonzero mean transverse velocity $\langle\kappa\rangle$ (Fig. 6), which depends strongly on the CW parameters.

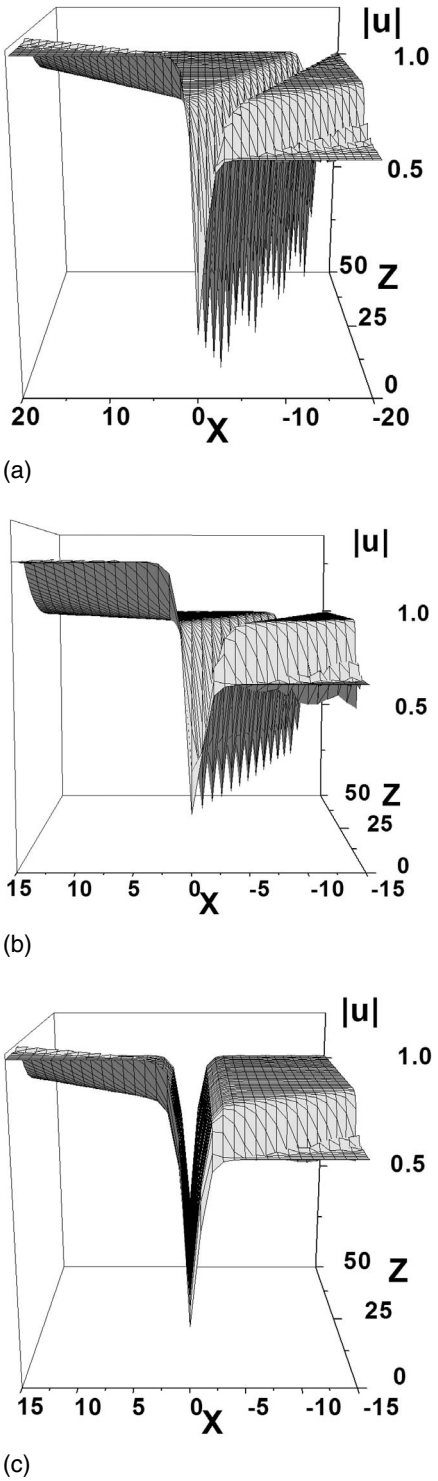

FIG. 8. Propagation of a dark soliton under the presence of a moderate perturbation due to a CW with amplitude $a=0.24$, transverse velocity $k_X=0$, and phase (a) $\phi=-\pi/4$, (b) $\phi=0$, and (c) $\phi=+\pi/4$.

As expected, the amplitude of the CW (a) can only determine the magnitude of the soliton mean transverse velocity, while the phase of the CW (ϕ) may affect both the direction and the magnitude of dark beam center displacement in a sinusoidal way (Fig. 7) with a constant phase period of 2π.

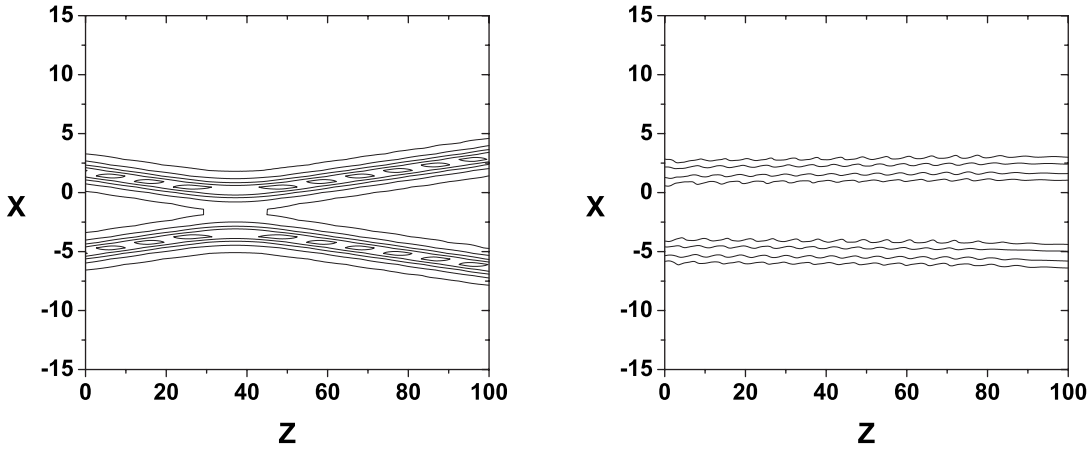

FIG. 9. Co-propagation of two dark (gray) solitons with initial positions $X_0^{(1,2)}=-5,1.71$, initial velocities $A^{(1,2)}=-0.05,+0.05$, and zero initial phase difference. The background is set to unity ($u_0=1$). (a) No CW is induced (homogeneous medium). (b) Collision suppression is achieved under the presence of a CW with $a=0.08$, $k_X=1$, and $\phi=0$.

The curve of Fig. 7 is antisymetric with respect to $(\langle k\rangle,\phi)=(0,\pi/4)$, while it remains unaffected when the initial beam center position varies ($X_0\neq 0$), as there is no transverse dependence on the CW-induced periodic potential [see Eq. (4) with $k_X=0$].

In order to compare the robustness of bright and dark spatial beams under the presence of a CW perturbation, we performed several numerical experiments by increasing the amplitude of the control signal up to $a=0.24$ and using different phase angles for the CW parameter ϕ. In all these cases, the system is strongly perturbed and cannot be considered as near-integrable. It is known that such problems lead to strong emission of radiation and excitation of nonlinear modes that cannot be described by any adiabatic approximation of the initial solution of the unperturbed problem (e.g., the beam or the pulse may be destroyed by the effect of moderate perturbation). Note that for the case of interaction between a bright soliton and a CW having such a large amplitude ($a=0.24$), the modulational instability of the background results in the formation of periodic series of secondary beams as shown in Figs. 2–4 of Ref. [30]. In our problem, as expected [2,4], the results show that dark beams exhibit significant robustness in comparison with their bright counterparts [30], as it can be seen in Fig. 8. In this case, the initial superposition of the CW and the dark soliton results in different asymptotic values of the total field amplitude due to the phase difference of the respective asymptotic values of the dark soliton ($\pm\pi$ at $\pm\infty$). However, in a short propagation distance and after emitting radiation, the beam transforms to a steadily breathing gray soliton having a constant and symmetric background and a nonzero mean transverse velocity.

III. TWO-SOLITON INTERACTIONS

In this section, we are focusing on the cases where interaction phenomena between two dark spatial solitons can be modified due to the presence of a CW in a controllable fashion. As mentioned above, dark solitons exhibit different interaction features with respect to their bright counterparts [4]. According to the results presented in the previous section, for the case of zero CW transverse velocity $k_X=0$, unlike bright soliton-PW interactions, the CW may lead to a qualitative differentiation of dark soliton interactions, as dark beams obtain nonzero transverse velocity even in cases where $k_X=0$. However, by using a CW control signal with nonzero transverse velocity, we may affect dark soliton interactions in a more flexible manner. Thus in the following examples we use CW-induced lattices with $k_X\neq 0$, while the dark soliton background is set to unity. The initial positions as well as the initial transverse velocities of both dark beams are selected appropriately in order to demonstrate the drastic effect of CW control signal on dark soliton interaction phenomena. All results are obtained by direct numerical integration of the original NLS equation by using as initial conditions the superposition of both dark beams and the CW. It is worth mentioning that the mutual interaction forces (repulsive for dark beams of opposite phase or attractive for dark beams with equal phase) between dark solitons are small as is well known [4]. As a result, we expect that the CW control signal will modify dark soliton interaction by affecting mainly the mean transverse velocity of each beam almost independently, so that we can utilize the analytical results, obtained for the single dark soliton case (Sec. II A).

The case of two dark solitons, initially located at $X_0^{(1),(2)}=(-5,1.71)$ with initial transverse velocities $A^{(1,2)}=(-0.05,+0.05)$, and equal (zero) initial phases, is shown in Fig. 9(a) propagating in a homogeneous (no CW is injected) defocusing medium. In this example, both dark beams (gray solitons) approach each other and elastic collision occurs after a short propagation distance. Note that the well-known bound state of two bright solitons does not apply to dark ones, while the dark soliton approach is mainly a result of the selection of nonzero initial beam transverse velocity (attraction forces are small). Hence in Fig. 9(a) after the collision point, dark beams evolve almost unaffected with opposite constant transverse velocities. However, the same beams in-

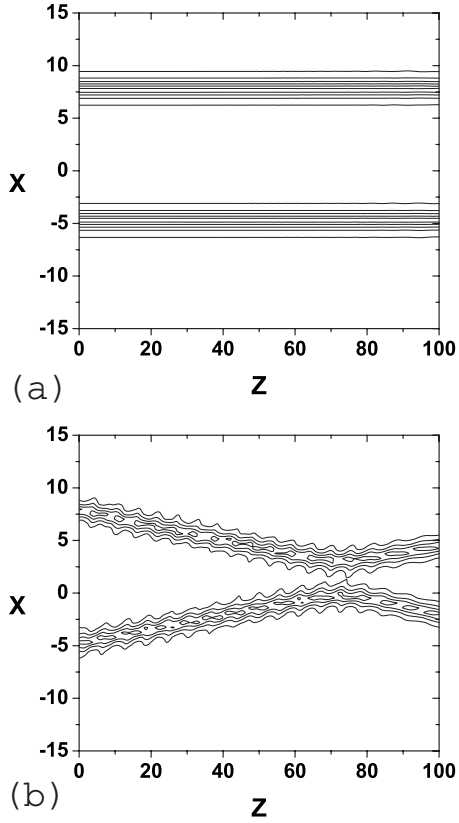

FIG. 10. Co-propagation of two dark (black) solitons with initial positions $X_0^{(1,2)}=-3\pi/2,5\pi/2$, zero initial transverse velocities, and initial phase difference π. The background is set to unity ($u_0=1$). (a) No CW is induced (homogeneous medium). (b) Symmetric soliton attraction is achieved under the presence of a CW with $a=0.1$, $k_X=1$, and $\phi=0$.

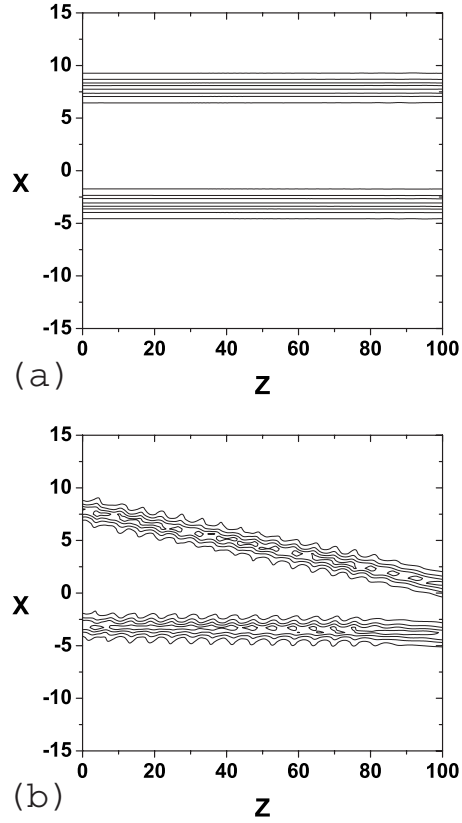

FIG. 11. Co-propagation of two dark (black) solitons with initial positions $X_0^{(1,2)}=-\pi,5\pi/2$, zero initial transverse velocities, and initial phase difference π. Background is set to unity ($u_0=1$). (a) No CW is induced (homogeneous medium). (b) Asymmetric soliton attraction is achieved under the presence of a CW with $a=0.1$, $k_X=1$, and $\phi=0$.

jected into a CW-induced photonic lattice, with CW parameters $a=0.08$, $k_X=1$, and $\phi=0$, may evolve almost unaffected as breathing gray solitons with zero mean transverse velocity, as can be seen in Fig. 9(b). It is noticeable, in this specific scenario, that collision suppression was easily achieved, as the control signal primarily altered the initial nonzero transverse velocity of both beams and second reduced the mutual soliton attraction force, which is small in general. On the other hand, in bright soliton interaction cases, the CW-induced potential had to balance the strong attraction forces between bright beams [31]. As a result, complete collision suppression of bright solitons may not lead to constant transverse velocity beam propagation; in the respective dark soliton collision suppression scenario, dark beams evolve with zero mean transverse velocity. Furthermore, by increasing the amplitude of the CW, we may not only prevent dark soliton collision, but induce soliton deviation (with opposite soliton velocities) as well.

Similarly to the case of bright soliton interactions, a CW control signal may cause symmetric (Fig. 10) or asymmetric (Fig. 11) dark soliton attraction depending strongly on the relative initial beam positions, with respect to the origin. Practically, by using a fixed CW with parameters $a=0.1$, $k_X=1$, and $\phi=0$, and injecting two well-separated black spatial beams with zero initial transverse velocities, we may control both soliton velocities almost simultaneously by varying appropriately their initial position. Note that in these examples (Figs. 10 and 11), the dark beams have an initial phase difference π [4]. Thus the repulsive force between them may be compensated by the CW control signal.

IV. SUMMARY AND CONCLUSIONS

In conclusion, dark spatial soliton dynamics in optically induced photonic lattices have been studied. The evolution of a dark beam has been shown to be affected drastically by the CW-induced potential, while the mean transverse velocity of the dark soliton has been shown to depend strongly on the parameters of the CW such as the amplitude, the transverse velocity, and the phase. This dependence suggests a dynamically reconfigurable control mechanism for beam steering and switching applications. Our analytical approach based on the variational perturbation method provided a dynamical system of the adiabatic evolution of the soliton parameters, and the results were shown to be in remarkable agreement with the direct numerical simulations.

In comparison with bright beams, dark solitons exhibit

qualitatively different evolution characteristics when propagating in CW-induced periodic lattices (e.g., robustness in strong CW perturbations). Moreover, the interaction of two solitons propagating in a CW-induced lattice has been investigated, and it has been shown that the features of the interaction can be determined by appropriate parameter selection for the CW, so that collisions can be enhanced or suppressed. Both results for spatial single- and two-dark soliton propagation are applicable to temporal dark solitons as well, while the results of the variational method may be directly extended in cases of dark soliton interaction with a PW control signal, forming a photonic lattice having a general periodic wave form.

The authors would like to thank the referee of this article for constructive comments and suggestions. The author I.T. acknowledges the project PENED 2003 co-financed by public expenditure through EC–European Social Fund (75%) and of public expenditure through Ministry of Development–General Secretariat of Research and Technology and through the private sector, under measure 8.3 of Operational Programme Competitiveness in the 3rd Community Support Programme (25%). All the authors acknowledge support of the research topic in its initial phase by the European Social Fund (75%) and National Resources (25%)–Operational Program for Educational and Vocational Training II (EPEAEK II) and particularly the Program PYTHAGORAS.

[1] A. Hasegawa and Y. Kodama, in *Solitons in Optical Communications, Oxford Series on Optical and Imaging Sciences*, edited by A. Hasegawa, M. Lapp, J. Nishizawa, B. B. Snavely, H. Stark, A. C. Tam, and T. Wilson (Clarendon Press, Oxford, 1995) Vol. 7.
[2] Y. S. Kivshar and B. Luther-Davies, Phys. Rep. **298**, 81 (1998).
[3] Y. S. Kivshar and G. P. Agrawal, in *Optical Solitons-From Fibers to Photonic Crystals*, edited by Y. S. Kivshar and G. Agrawal (Academic Press, New York, 2003).
[4] W. Zhao and E. Bourkoff, Opt. Lett. **14**, 1371 (1989)
[5] V. E. Zakharov Shabat, Zh. Eksp. Teor. Fiz. **64**, 1627 (1973); [Sov. Phys. JETP **37**, 823 (1973)].
[6] K. J. Blow and N. J. Doran, Phys. Lett. **107A**, 55 (1985).
[7] Y. S. Kivshar and X. Yang, Phys. Rev. E **49**, 1657 (1994).
[8] V. V. Konotop and V. E. Vekslerchik, Phys. Rev. E **49**, 2397 (1994).
[9] X. Chen, Z. Chen, and N. Huang, J. Phys. A **31**, 6929 (1998).
[10] X. Chen and Z. Chen, IEEE J. Quantum Electron. **34**, 1308 (1998).
[11] N. Huang, S. Chi, and X. Chen, J. Phys. A **32**, 3939 (1999).
[12] S. Ao and J. Yan, J. Phys. A **38**, 2399 (2005).
[13] S. Ao and J. Yan, J. Phys. A **39**, 1979 (2006).
[14] T. Yan, H. Cai, and N. Huang, J. Phys. A **39**, 9493 (2006).
[15] Y. S. Kivshar and W. Krolikowski, Opt. Commun. **114**, 353 (1995).
[16] V. M. Lashkin, Phys. Rev. E **70**, 066620 (2004).
[17] A. A. Sukhorukov, Y. S. Kivshar, H. S. Eisenberg, and Y. Silberberg, IEEE J. Quantum Electron. **39**, 31 (2003).
[18] Y. S. Kivshar, W. Krolikowski, and O. A. Chubykalo, Phys. Rev. E **50**, 5020 (1994).
[19] W. Krolikowski and Y. S. Kivshar, J. Opt. Soc. Am. B **13**, 876 (1996).
[20] M. Johansson and Y. S. Kivshar, Phys. Rev. Lett. **82**, 85 (1999).
[21] V. V. Konotop and S. Takeno, Phys. Rev. E **60**, 1001 (1999).
[22] J. W. Fleischer, G. Bartal, O. Cohen, T. Schwartz, O. Manela, B. Freedman, M. Segev, H. Buljan, and N. K. Efremidis, Opt. Express **13**, 1780 (2005).
[23] R. Morandotti, H. S. Eisenberg, Y. Silberberg, M. Sorel, and J. S. Aitchison, Phys. Rev. Lett. **86**, 3296 (2001).
[24] J. W. Fleischer, T. Carmon, M. Segev, N. K. Efremidis, and D. N. Christodoulides, Phys. Rev. Lett. **90**, 023902 (2003).
[25] D. Mandelik, R. Morandotti, J. S. Aitchison, and Y. Silberberg, Phys. Rev. Lett. **92**, 093904 (2004).
[26] N. K. Efremidis, S. Sears, D. N. Christodoulides, J. W. Fleischer, and M. Segev, Phys. Rev. E **66**, 046602 (2002).
[27] E. P. Fitrakis, P. G. Kevrekidis, H. Susanto, and D. J. Frantzeskakis, Phys. Rev. E **75**, 066608 (2007).
[28] Y. Kominis and K. Hizanidis, J. Opt. Soc. Am. B **21**, 562 (2004).
[29] Y. Kominis and K. Hizanidis, J. Opt. Soc. Am. B **22**, 1360 (2005).
[30] Y. Kominis and K. Hizanidis, Opt. Commun. **234**, 193 (2004).
[31] I. Tsopelas, Y. Kominis, and K. Hizanidis, Phys. Rev. E **74**, 036613 (2006).
[32] G. Theocharis, P. Schmelcher, M. K. Oberthaler, P. G. Kevrekidis, and D. J. Frantzeskakis, Phys. Rev. A **72**, 023609 (2005).